


Identification of immunomodulatory hub genes and cell signatures in mouse lungs exposed to cigarette smoke: An integrated bioinformatic analysis using StringDB, Cytoscape, and ImmuneCellAI

Meena Easwaran¹

¹McWilliams School of Biomedical Informatics, The University of Texas Health Science Center, Houston

December 04, 2024

Author Note

Meena Easwaran  <https://orcid.org/0009-0007-0377-748X>

The data set "GSE76205" used in this research was sourced from the National Center for Biotechnology Information Gene Expression Omnibus (NCBI GEO). I have no conflicts of interest to report. This article will not be submitted for publication in any scientific journal.

For inquiries related to this article, please reach out to Meena Easwaran at the McWilliams School of Biomedical Informatics, The University of Texas Health Science Center, 7000 Fannin St, Suite 600, Houston, TX 77030. Email: meena.easwaran@uth.tmc.edu.

Abstract

Cigarette smoke (CS) exposure induces significant changes that have lasting effects on the structural, cellular, and molecular dynamics of lung tissues. This study analyzed the temporal variations in gene expression in mouse lungs subjected to different durations of CS exposure, ranging from one day to nine months, focusing on differentially expressed genes (DEGs), pathway enrichment, and immune-related hub gene identification using a publicly available RNA sequencing dataset. Differential expression analysis showed minimal alterations, with eight DEGs identified after one day, increasing dramatically to 1,031 DEGs at seven days. Over time, the number of DEGs decreased, with only nine at one month, 190 at three months, 121 at six months, and 677 at nine months, indicating fluctuating transcriptomic responses. Functional enrichment analysis through Gene ontology (GO) and the Kyoto Encyclopedia of Genes and Genomes (KEGG) pathway database highlighted significant immune response modulation, particularly at six- and nine-months post-exposure. Key enriched pathways included inflammation, cytokine production, chemotaxis, and extracellular matrix interactions. Network analysis identified crucial hub genes linked to inflammatory responses (Gpx1, Nlrp3, Il1r1), cytokine production (Il1a and Ptgs2), as well as cell migration and chemotaxis (Serpine1 and Pecam1). Furthermore, immune cell profiling showed transient increases in immune cell infiltration after one day of exposure, stabilizing in later periods, suggesting potential immunosuppression with prolonged exposures. Overall, these findings underscore the evolving immune landscape and tissue remodeling associated with chronic CS exposure, highlighting potential molecular targets for addressing smoking-related lung diseases.

Keywords: Cigarette smoke, mouse lungs, Differential Gene Expression, Pathway database enrichment, network analysis

Introduction

Cigarette smoke (CS) significantly affects respiratory health, impacting various parts of the respiratory system, such as the nasal cavity (Hadar et al., 2009; Pagliuca et al., 2015), pharynx (Garcia Martins et al., 2012; Moore, 1971; Radsel & Kambe, 1978), larynx (Easwaran et al., 2021, 2022; Erickson-DiRenzo et al., 2020, 2021; Moore, 1971; R. A. Renne & Gideon, 2006), and lungs (Curtin et al., 2004; Phillips et al., 2015; R. Renne et al., 2009; Walser et al., 2008). CS contains thousands of toxic substances, including carcinogens, which can trigger and worsen a range of respiratory diseases upon inhalation (Centers for Disease Control and Prevention, 2010; Services et al., 2014). The first area exposed to CS, the nasal region, is most susceptible to chronic rhinosinusitis and nasal congestion (Reh et al., 2012). Furthermore, long-term irritation and inflammation of the nasal mucosa can elevate the likelihood of developing nasal tumors (Vineis et al., 2004). CS exposure can also negatively impact the pharynx and larynx, leading to conditions like pharyngitis, laryngitis, Reinke's edema, and cancers with prolonged exposure (Easwaran et al., 2021, 2022; Erickson-DiRenzo et al., 2020, 2021; Garcia Martins et al., 2012; Moore, 1971; R. A. Renne & Gideon, 2006).

The harmful impacts of CS become more evident as they extend into the lower airways, especially in the lungs. Chronic obstructive pulmonary disease (COPD), a major cause of global death, often results from extended exposure to CS (Laniado-Laborin, 2009; Song et al., 2021). Individuals with COPD display symptoms such as chronic bronchitis and emphysema (Petrache & Serban, 2023). Chronic bronchitis involves inflammation and increased mucus production in the bronchi, leading to ongoing coughing (Kim & Criner, 2013; Widysanto & Mathew, 2022). In emphysema, the lung tissue deteriorates due to the enlargement of the air sacs or alveoli, hindering airflow and diminishing lung capacity (Mouronte-Roibás et al., 2016; Petrache &

Serban, 2023). There is also a markedly higher risk of lung cancer among those who are repeatedly exposed to CS (Abelia et al., 2023; Walser et al., 2008).

CS not only compromises the structural integrity of lung tissue but also disrupts the immune mechanisms. Following exposure to CS, immune cells in the lungs, including macrophages, neutrophils, and T cells, undergo significant alterations in their functional capabilities (Lee et al., 2012; Sopori, 2002; Strzelak et al., 2018). This results in chronic inflammation, diminished efficacy in pathogen clearance, and an increased susceptibility to infections. Such immune dysregulation contributes to a persistent cycle of lung tissue damage and repair, exacerbating conditions such as COPD and facilitating oncogenic transformations. Understanding the immune system's responses to CS exposure is imperative, as immune cells are pivotal to the lung's defense processes. Furthermore, focusing on immune mechanisms yields valuable insights into potential therapeutic targets that could alleviate CS-induced lung diseases.

Investigating the immune responses by examining time-related temporal dynamics offers valuable insights into the differing impacts of acute and chronic CS exposure on the immune system. Temporal analysis facilitates the identification of initial immune alterations, adaptive responses, and long-term pathological changes, enhancing our understanding of how sustained CS exposure contributes to chronic pulmonary conditions. Mouse models serve as an excellent experimental resource for this type of analysis due to their analogous immune responses and disease progression mechanisms that often reflect those observed in humans (Medicine & Bryda, 2013; Walrath et al., 2010). These models support controlled, long-term investigations that are both ethically and practically challenging in human subjects, thereby enabling the discovery of early biomarkers and potential therapeutic targets.

One noteworthy study by Miller et al. (2017) evaluates genetic and metabolic alterations in mice lungs exposed to CS for periods of one or seven days and three, six, or nine months using bulk RNA sequencing, establishing various time points for analysis. However, despite the comprehensive nature of this study, it does not include a thorough examination of immune cell-specific signatures or the identification of immunomodulatory hub genes or key regulatory agents responsible for driving immune dysregulation. Addressing this deficiency is essential, as understanding the specific involvement of immune cells and critical regulatory molecules could provide new insights into the pathology associated with CS exposure. In this context, this study aims to bridge this scientific gap by employing advanced bioinformatics tools, including Metascape (Zhou et al., 2019) for gene ontology (GO) (Ashburner et al., 2000) and pathway database enrichment, alongside StringDB (Szklarczyk et al., 2023) and Cytoscape (Shannon et al., 2003) for network analysis. This approach will facilitate the identification of crucial hub genes and immune cell signatures, thereby providing a comprehensive understanding of the immune landscape in lungs subjected to CS exposure over time.

Materials and Methods

Data retrieval

The bulk RNA sequencing dataset from Miller et al. (2017) was employed in this study. The dataset was obtained from the National Center for Biotechnology Information Gene Expression Omnibus (NCBI GEO) (Barrett et al., 2013) using the search query "cigarette smoke and lungs," which facilitated the identification of the relevant dataset with the accession ID "GSE76205". The identified dataset was analyzed using the NIH LINCS tool known as "GREIN" (GEO RNA-seq Experiments Interactive Navigator) (Mahi et al., 2019) to retrieve both raw and normalized data counts. This data series comprised gene expression profiles from

mouse lungs subjected to CS exposure and those exposed to air as controls, recorded at various time points: one day, seven days, and three, six, or nine months. Regarding sample sizes, on day one, there were five samples from the control group and four from the CS-exposed group. At seven days, both control and CS-exposed groups had five samples each. For the one-month and three-month intervals, the sample sizes remained consistent at five for each group. The control group comprised four samples at six and nine months, while the CS-exposed group included five.

Differential expression analysis

Differential expression analysis was performed to compare gene expression profiles between the CS-exposed and air-exposed control groups at each experimental time point. This analysis used the "DESeq2" package (Love et al., 2014) within the R programming language. The threshold for determining statistically significant differentially expressed genes (DEGs) was established at a false discovery rate (FDR) of ≤ 0.05 and a |fold change| greater than 1.5. The DEGs that met these statistical significance criteria were subsequently represented as volcano plots utilizing the "EnhancedVolcano" R package (*Bioconductor - EnhancedVolcano*, n.d.). It is important to note that rows exhibiting low gene counts (i.e., <10) were excluded before performing the differential expression analysis.

Functional enrichment analysis

The significant DEGs from the comparisons between the CS and the control groups at each time point were subjected to a comparative functional enrichment analysis utilizing Metascape (Zhou et al., 2019). This enrichment analysis focused on the GO categories of biological processes, cellular compartments, and molecular functions (Ashburner et al., 2000), as well as the Kyoto Encyclopedia of Genes and Genomes (KEGG) pathway database (Kanehisa, 2019; Kanehisa et al., 2023; Kanehisa & Goto, 2000). The criteria for significance in each

enriched term included a minimum gene overlap of three, a p-value cutoff of 0.05, and a minimum enrichment factor of 1.5. The p-values from the Metascape enrichments were adjusted using the Benjamini-Hochberg method (Jafari & Ansari-Pour, 2019). Comparative enrichments across each time point were visualized through a heatmap.

Hub gene identification via network analysis

All DEGs associated with specific immune cell mechanisms were visualized as bigger protein-protein interaction (PPI) networks using StringDB version 12 (<https://string-db.org/>) (Szkarczyk et al., 2023). These bigger PPIs were exported to the Cytoscape platform (Shannon et al., 2003) to identify the hub genes or key regulatory genes. Within the platform, the Maximal clique centrality (MCC) algorithm (Li & Xu, 2019) from the cytoHubba plugin (Chin et al., 2014) was utilized to determine the top ten hub genes in each PPI.

ImmuneCellAI analysis

The composition of immune cells in the lung tissue of mice exposed to CS was analyzed utilizing ImmuneCellAI-mouse (<https://guolab.wchscu.cn/ImmuCellAI-mouse/#!/>) (Miao et al., 2022), a computational tool designed to determine immune cell types from gene expression data. Input was derived from normalized gene expression counts obtained from GREIN (Mahi et al., 2019). The relative immune cell abundance scores across different experimental conditions from this analysis were subsequently employed for statistical evaluations using GraphPad Prism version 10.4. These evaluations aimed to investigate the temporal dynamics of immune cell infiltration in the lungs of CS-exposed mice. A two-way analysis of variance (ANOVA) test, accompanied by a post-hoc Tukey multiple comparison test, was conducted to analyze the data.

Results

Differential expression analysis

Differential expression analysis revealed eight DEGs between the one-day CS-exposed and the control groups, as shown in Figure 1 (see Appendix B). Specifically, five genes were upregulated, while three were downregulated in response to CS exposure. On day seven, the analysis identified 1,031 DEGs, comprising 491 upregulated and 540 downregulated genes between both groups, as seen in Figure 1 (see Appendix B). After one month of exposure, nine DEGs, consisting of two upregulated and seven downregulated genes, were detected, as depicted in Figure 2 (see Appendix B). The analysis identified 190 DEGs at three months, with 90 being upregulated and 100 downregulated, as illustrated in Figure 2 (see Appendix B). Following six months of CS exposure, 121 DEGs were identified, including 92 upregulated and 29 downregulated genes, as shown in Figure 3 (see Appendix B). At nine months, the total number of DEGs increased to 677, composed of 312 upregulated and 365 downregulated genes across both groups, as seen in Figure 3 (see Appendix B).

Functional enrichment analysis

GO and KEGG pathway database comparative functional enrichment analysis of significant DEGs across all experimental time points revealed substantial modulation of various biological mechanisms, remarkably immune cell functions, and mechanisms at the longer time points of six- and nine-months following CS exposure, as illustrated in Figure 4 (see Appendix B). Specifically, alterations in the extracellular matrix (ECM), immune receptor activity, lymphocyte activation, positive regulation of cell migration, cytokine production, regulation of chemotaxis, and regulation of inflammatory responses were observed. The genes enriched in these categories are detailed in Table 1 (refer to Appendix A). Also, it is noteworthy that earlier time points did not exhibit significant immune modulation, apart from specific responses noted on day seven post-CS exposure.

Network-based hub gene analysis

The top ten hub genes identified in the inflammatory response PPI on Cytoscape were Gpx1 - Glutathione peroxidase 1, Gpx2 - Glutathione peroxidase 2, Ptgs2 - Prostaglandin-endoperoxide synthase 2, Ccr2 - C-C motif chemokine receptor 2, Nlrp3 - NOD-like receptor protein 3, Mefv - Mediterranean fever gene, Il1r1 - Interleukin 1 receptor type 1, Nod2 - Nucleotide-binding oligomerization domain containing 2, Tlr9 - Toll-like receptor 9, and Il10ra - Interleukin 10 receptor subunit alpha, as shown in Figure 5 (see Appendix B). Hub genes associated with the cytokine production included Ptgs2, Il1r1, Il1a - Interleukin 1 alpha, Ccr2, Ptpcr - Protein tyrosine phosphatase receptor type C, Tlr9 - Toll-like receptor 9, Syk - Spleen tyrosine kinase, Il6ra - Interleukin 6 receptor subunit alpha, Ccr7 - C-C motif chemokine receptor 7, and Cd40lg - CD40 ligand, as demonstrated in Figure 5 (see Appendix B).

In terms of chemotaxis and cell migration, Il1a, Serpine1 - Serpin family E member 1, Pecam1 - Platelet and endothelial cell adhesion molecule 1, Fn1 - Fibronectin 1, Thbs1 - Thrombospondin 1, Fgf16 - Fibroblast growth factor 16, Fgf10 - Fibroblast growth factor 10, Edn1 - Endothelin 1, Pdgfrb - Platelet-derived growth factor receptor beta, Pdgfra - Platelet-derived growth factor receptor alpha, Egfr - Epidermal growth factor receptor, Ptgs2, and Myc - MYC proto-oncogene were the identified hub genes as shown in Figure 6 (see Appendix B). Furthermore, Ccl25 - C-C motif chemokine ligand 25, Ccl12 - C-C motif chemokine ligand 12, Cxcl15 - C-X-C motif chemokine ligand 15, Ccr2, Ccr6 - C-C motif chemokine receptor 6, Cxcl3 - C-X-C motif chemokine ligand 3, Cxcl5 - C-X-C motif chemokine ligand 5, Cxcr1 - C-X-C motif chemokine receptor 1, Ccr7 - C-C motif chemokine receptor 7, and Ppbp - Pro-platelet basic protein were the immune receptor activity related hub genes, as seen in Figure 7 (see Appendix B). Genes Cd40lg, Ptpcr, and Ccr7 are also critical hub genes in lymphocyte

activation along with other genes including *Klrb1c* - Killer cell lectin-like receptor subfamily B member 1C, *Itgam* - Integrin subunit alpha M (also known as CD11b), *Il7r* - Interleukin 7 receptor, *Il2rb* - Interleukin 2 receptor subunit beta, *Klrk1* - Killer cell lectin-like receptor subfamily K member 1 (also known as NKG2D), *Prf1* - Perforin 1, and *Il2rg* - Interleukin 2 receptor subunit gamma, as displayed in Figure 7 (see Appendix B).

ECM, as visualized in Figure 8 (see Appendix B), was another immunomodulatory mechanism observed, which included the following hub genes: *Lox1* - Lectin-like oxidized low-density lipoprotein receptor-1, *Col3a1* - Collagen type III alpha 1 chain, *Fn1*, *Col4a1* - Collagen type IV alpha 1 chain, *Col5a1* - Collagen type V alpha 1 chain, *Col5a2* - Collagen type V alpha 2 chain, *Ccn2* - Cellular communication network factor 2 (also known as connective tissue growth factor, CTGF), *Lox* - Lysyl oxidase, *Col1a1* - Collagen type I alpha 1 chain, and *Fbn1* - Fibrillin 1.

Immune cell profiling using ImmuneCellAI-mouse

The immune cell composition, including B cells, dendritic cells, granulocytes, macrophages, monocytes, natural killer (NK) cells, and T cells, was evaluated using the normalized expression dataset obtained from GREIN. The results showed no notable variations in cell composition across different durations of CS exposure—namely, one day, seven days, and three, six, or nine months, as illustrated in Figure 9 (see Appendix B). The analysis of estimated immune cell infiltration scores demonstrated a transient rise after one day of CS exposure, which decreased with prolonged exposures, indicating a possible immunosuppressive response.

Discussion

Investigation into the temporal dynamics of immune responses in the context of CS exposure is paramount for elucidating the complex pathways contributing to the onset and

progression of pulmonary diseases. This study employed a publicly available RNA sequencing dataset (Miller et al., 2017) to analyze immune responses over varying durations of CS exposure. The findings illustrate a significant trajectory of gene expression alterations and shifts in immune modulation, revealing a transition from initial immune activation to chronic suppression as exposure time extends.

Differential expression and functional enrichment analysis demonstrated a biphasic response to CS exposure. Acute exposure, particularly at seven days, was marked by significant differential expression and enrichment of inflammatory and immune-related pathways, including cytokine production, chemotaxis, and immune receptor activity, reflecting an immediate innate immune response to tissue damage. These findings are consistent with the known rapid arrival of inflammatory cells at injury sites, typically within days of an external insult like CS (Koh & DiPietro, 2011; Park et al., 2020). Immune cell infiltration scores from ImmuneCellAI further corroborated this pattern, showing an initial spike in immune cell recruitment at acute exposure timelines, followed by a decline with prolonged exposure, suggesting the onset of an immunosuppressive environment.

Interestingly, differential expression and immune and inflammation-related pathway enrichments diminished at intermediate time points of one and three months before re-emerging at six and nine months. The intermediate phase may reflect subtle shifts in immune activity and tissue remodeling, indicating an adaptive response by the lung to sustained CS exposure. This phase of temporary stabilization could signify a balance between repair mechanisms and inflammation as part of the adaptation process. However, with continued exposure, these adaptive processes may have become overwhelmed, leading to a resurgence of immune and ECM-related pathway enrichment, as reported after six and nine months of exposure in this

study. In human lungs, CS exposure has been shown to induce ECM-associated genes, but not inflammatory or immune-related genes, resembling characteristics of COPD that develop over the long term (Oberholte et al., 2021). In this study, it is plausible that at the later time points identified, specifically at six and nine months, the enriched ECM and immune/inflammatory pathways may demonstrate similar perturbations. These pathways could evolve from their initial transient responses toward pathological remodeling and immunosuppression. Such alterations can induce carcinogenic and infectious conditions over time (Gu et al., 2018; Laniado-Laborin, 2009; Lee et al., 2012; Mouronte-Roibás et al., 2016; Strzelak et al., 2018). While the current bioinformatic methodologies used in this study provide valuable insights into the enriched pathways involved in the possible dual role of CS-induced responses—shifting from protective to pathological over time—they fall short of clarifying the directionality of pathway activation or inactivation. Therefore, further research is vital to explore these mechanistic nuances and validate the proposed hypotheses regarding the underlying responses.

The network analysis provided valuable insights into the regulatory hub genes underlying these mechanisms. Genes such as *Ptgs2*, *Nlrp3*, and *Il1r1* were central to inflammatory responses, while *Fn1*, *Col1a1*, and *Lox* were pivotal in ECM remodeling. The functional roles of these genes suggest their potential utility in precision medicine. For instance, *Ptgs2* could serve as a therapeutic target for mitigating lung inflammation (Nelin et al., 2022), while *Nlrp3* and its downstream signaling may represent biomarkers for early detection of chronic inflammatory states (Chen et al., 2023). Similarly, genes involved in ECM integrity, like *Fn1*, could inform therapeutic strategies (Spada et al., 2021) to prevent fibrosis and tissue remodeling. Future studies should investigate these hub genes to validate their roles and explore their potential in biomarker development and therapeutic targeting.

Despite the noteworthy findings presented in this study, several limitations must be acknowledged. The reliance on bulk RNA sequencing datasets constrains the ability to identify cell-specific transcriptional alterations. Implementing single-cell RNA sequencing or spatial transcriptomics could offer enhanced resolution regarding immune cell dynamics and their interactions within the lung microenvironment affected by CS exposure. Furthermore, while the findings are insightful, the reliance on murine models necessitates careful extrapolation to human disease contexts, considering the interspecies variations in immune responses and lung architecture. It is imperative to validate these findings in human cohorts or advanced organoid models to ensure their translational relevance. Lastly, upcoming research should also consider sex-specific differences and environmental co-exposures, such as air pollution, as these factors may further influence the immune and transcriptional responses observed.

Conclusion

This study provides a comprehensive examination of the evolution of immune responses, inflammation, and ECM remodeling in mouse lungs following exposure to CS, utilizing transcriptomic analysis. It highlights significant molecular components and pathways that evolve from acute immune activation to chronic immune dysregulation or immunosuppression. The results emphasize the necessity of temporal analysis for a deeper understanding of pulmonary and other respiratory disease mechanisms and for identifying potential biomarkers and therapeutic targets. By incorporating precision medicine strategies and validating findings in human models, future research may facilitate the development of targeted interventions aimed at alleviating the adverse effects of CS on respiratory health.

Acknowledgments

I thank Professors Debora Simmons and Xiaoqian Jiang for their exceptional teaching and support throughout this course. I also thank Professor Lex Frieden and Teaching Assistant Liat Shoham from the BMI 6313: Scientific Writing in Healthcare course at the McWilliams School of Biomedical Informatics for their instruction and guidance in scientific writing.

References

- Abelia, X. A., Lesmana, R., Goenawan, H., Abdulah, R., & Barliana, M. I. (2023). Comparison impact of cigarettes and e-cigs as lung cancer risk inductor: a narrative review. *European Review for Medical and Pharmacological Sciences*, 27(13), 6301–6318.
https://doi.org/10.26355/EURREV_202307_32990
- Ashburner, M., Ball, C. A., Blake, J. A., Botstein, D., Butler, H., Cherry, J. M., Davis, A. P., Dolinski, K., Dwight, S. S., Eppig, J. T., Harris, M. A., Hill, D. P., Issel-Tarver, L., Kasarskis, A., Lewis, S., Matese, J. C., Richardson, J. E., Ringwald, M., Rubin, G. M., & Sherlock, G. (2000). Gene Ontology: tool for the unification of biology. *Nature Genetics* 2000 25:1, 25(1), 25–29. <https://doi.org/10.1038/75556>
- Barrett, T., Wilhite, S. E., Ledoux, P., Evangelista, C., Kim, I. F., Tomashevsky, M., Marshall, K. A., Phillippy, K. H., Sherman, P. M., Holko, M., Yefanov, A., Lee, H., Zhang, N., Robertson, C. L., Serova, N., Davis, S., & Soboleva, A. (2013). NCBI GEO: archive for functional genomics data sets—update. *Nucleic Acids Research*, 41(D1), D991–D995.
<https://doi.org/10.1093/NAR/GKS1193>
- Bioconductor - EnhancedVolcano*. (n.d.). Retrieved April 24, 2024, from <https://bioconductor.org/packages/release/bioc/html/EnhancedVolcano.html>
- Centers for Disease Control and Prevention, N. C. for C. D. P. and H. P. O. on S. and H. (2010). How Tobacco Smoke Causes Disease: The Biology and Behavioral Basis for Smoking-Attributable Disease: A Report of the Surgeon General. Atlanta (GA): Centers for Disease Control and Prevention (US). In *How Tobacco Smoke Causes Disease: The Biology and Behavioral Basis for Smoking-Attributable Disease: A Report of the Surgeon General*.

Centers for Disease Control and Prevention (US).

<https://www.ncbi.nlm.nih.gov/books/NBK53017/>

Chen, Y., Ye, X., Escames, G., Lei, W., Zhang, X., Li, M., Jing, T., Yao, Y., Qiu, Z., Wang, Z., Acuña-Castroviejo, D., & Yang, Y. (2023). The NLRP3 inflammasome: contributions to inflammation-related diseases. *Cellular & Molecular Biology Letters*, 28(1), 51.

<https://doi.org/10.1186/S11658-023-00462-9>

Chin, C. H., Chen, S. H., Wu, H. H., Ho, C. W., Ko, M. T., & Lin, C. Y. (2014). cytoHubba: Identifying hub objects and sub-networks from complex interactome. *BMC Systems Biology*, 8(4), 1–7. <https://doi.org/10.1186/1752-0509-8-S4-S11/TABLES/4>

Curtin, G. M., Higuchi, M. A., Ayres, P. H., Swauger, J. E., & Mosberg, A. T. (2004). Lung tumorigenicity in A/J and rasH2 transgenic mice following mainstream tobacco smoke inhalation. *Toxicological Sciences*, 81(1), 26–34. <https://doi.org/10.1093/toxsci/kfh175>

Easwaran, M., Martinez, J. D., Kim, J. B., & Erickson-DiRenzo, E. (2022). Modulation of mouse laryngeal inflammatory and immune cell responses by low and high doses of mainstream cigarette smoke. *Scientific Reports* 2022 12:1, 12(1), 1–19. <https://doi.org/10.1038/s41598-022-23359-7>

Easwaran, M., Martinez, J. D., Ramirez, D. J., Gall, P. A., & Erickson-DiRenzo, E. (2021). Short-term whole body cigarette smoke exposure induces regional differences in cellular response in the mouse larynx. *Toxicology Reports*, 8, 920–937.

<https://doi.org/10.1016/J.TOXREP.2021.04.007>

Erickson-DiRenzo, E., Easwaran, M., Martinez, J. D., Dewan, K., & Sung, C. K. (2021). Mainstream Cigarette Smoke Impacts the Mouse Vocal Fold Epithelium and Mucus Barrier. *The Laryngoscope*, 131(11), 2530–2539. <https://doi.org/10.1002/LARY.29572>

Erickson-DiRenzo, E., Singh, S. P., Martinez, J. D., Sanchez, S. E., Easwaran, M., & Valdez, T.

A. (2020). Cigarette smoke-induced changes in the murine vocal folds: A Raman spectroscopic observation. *Analyst*, 145(23), 7709–7717.

<https://doi.org/10.1039/d0an01570a>

Garcia Martins, R. H., Marques Madeira, S. L., Fabro, A. T., Rocha, N. D. S., De Oliveira

Semenzati, G., & Alves, K. F. (2012). Effects to exposure of tobacco smoke and alcohol on the tongue and pharynx of rats. *Inhalation Toxicology*, 24(3), 153–160.

<https://doi.org/10.3109/08958378.2011.649190>

Gu, B. H., Madison, M. C., Corry, D., & Kheradmand, F. (2018). Matrix remodeling in chronic lung diseases. *Matrix Biology*, 73, 52–63. <https://doi.org/10.1016/J.MATBIO.2018.03.012>

Hadar, T., Yaniv, E., Shvili, Y., Koren, R., & Shvero, J. (2009). Histopathological changes of the nasal mucosa induced by smoking Smoking-induced nasal mucosa changes. *Inhalation Toxicology*, 21(13), 1119–1122. <https://doi.org/10.3109/08958370902767070>

Jafari, M., & Ansari-Pour, N. (2019). Why, When and How to Adjust Your P Values? *Cell Journal (Yakhteh)*, 20(4), 604. <https://doi.org/10.22074/CELLJ.2019.5992>

Kanehisa, M. (2019). Toward understanding the origin and evolution of cellular organisms. *Protein Science*, 28(11), 1947–1951. <https://doi.org/10.1002/PRO.3715>

Kanehisa, M., Furumichi, M., Sato, Y., Kawashima, M., & Ishiguro-Watanabe, M. (2023). KEGG for taxonomy-based analysis of pathways and genomes. *Nucleic Acids Research*, 51(D1), D587–D592. <https://doi.org/10.1093/NAR/GKAC963>

Kanehisa, M., & Goto, S. (2000). KEGG: Kyoto Encyclopedia of Genes and Genomes. *Nucleic Acids Research*, 28(1), 27–30. <https://doi.org/10.1093/NAR/28.1.27>

- Kim, V., & Criner, G. J. (2013). Chronic Bronchitis and Chronic Obstructive Pulmonary Disease. *American Journal of Respiratory and Critical Care Medicine*, 187(3), 228. <https://doi.org/10.1164/RCCM.201210-1843CI>
- Koh, T. J., & DiPietro, L. A. (2011). Inflammation and wound healing: The role of the macrophage. *Expert Reviews in Molecular Medicine*, 13, e23. <https://doi.org/10.1017/S1462399411001943>
- Laniado-Laborin, R. (2009). Smoking and Chronic Obstructive Pulmonary Disease (COPD). Parallel Epidemics of the 21st Century. *International Journal of Environmental Research and Public Health*, 6(1), 209. <https://doi.org/10.3390/IJERPH6010209>
- Lee, J., Taneja, V., & Vassallo, R. (2012). Cigarette Smoking and Inflammation: Cellular and Molecular Mechanisms. *Journal of Dental Research*, 91(2), 142. <https://doi.org/10.1177/0022034511421200>
- Li, C., & Xu, J. (2019). Feature selection with the Fisher score followed by the Maximal Clique Centrality algorithm can accurately identify the hub genes of hepatocellular carcinoma. *Scientific Reports*, 9(1), 1–11. <https://doi.org/10.1038/s41598-019-53471-0>
- Love, M. I., Huber, W., & Anders, S. (2014). Moderated estimation of fold change and dispersion for RNA-seq data with DESeq2. *Genome Biology*, 15(12), 1–21. <https://doi.org/10.1186/S13059-014-0550-8/FIGURES/9>
- Mahi, N. Al, Najafabadi, M. F., Pilarczyk, M., Kouril, M., & Medvedovic, M. (2019). GREIN: An Interactive Web Platform for Re-analyzing GEO RNA-seq Data. *Scientific Reports*, 9(1). <https://doi.org/10.1038/S41598-019-43935-8>
- Medicine, M., & Bryda, E. C. (2013). The Mighty Mouse: The Impact of Rodents on Advances in Biomedical Research. *Missouri Medicine*, 110(3), 207. [/pmc/articles/PMC3987984/](https://pubmed.ncbi.nlm.nih.gov/23987984/)

- Miao, Y. R., Xia, M., Luo, M., Luo, T., Yang, M., & Guo, A. Y. (2022). ImmuCellAI-mouse: a tool for comprehensive prediction of mouse immune cell abundance and immune microenvironment depiction. *Bioinformatics*, 38(3), 785–791.
<https://doi.org/10.1093/BIOINFORMATICS/BTAB711>
- Miller, M. A., Danhorn, T., Cruickshank-Quinn, C. I., Leach, S. M., Jacobson, S., Strand, M. J., Reisdorph, N. A., Bowler, R. P., Petrache, I., & Kechris, K. (2017). Gene and metabolite time-course response to cigarette smoking in mouse lung and plasma. *PLoS ONE*, 12(6), e0178281. <https://doi.org/10.1371/JOURNAL.PONE.0178281>
- Moore, C. (1971). Cigarette Smoking and Cancer of the Mouth, Pharynx, and Larynx: A Continuing Study. *JAMA*, 218(4), 553–558.
<https://doi.org/10.1001/JAMA.1971.03190170031005>
- Mouronte-Roibás, C., Leiro-Fernández, V., Fernández-Villar, A., Botana-Rial, M., Ramos-Hernández, C., & Ruano-Ravina, A. (2016). COPD, emphysema and the onset of lung cancer. A systematic review. *Cancer Letters*, 382(2), 240–244.
<https://doi.org/10.1016/J.CANLET.2016.09.002>
- Nelin, L. D., Jin, Y., Chen, B., Liu, Y., Rogers, L. K., & Reese, J. (2022). Cyclooxygenase-2 deficiency attenuates lipopolysaccharide-induced inflammation, apoptosis, and acute lung injury in adult mice. *American Journal of Physiology - Regulatory Integrative and Comparative Physiology*, 322(2), R126–R135.
https://doi.org/10.1152/AJPREGU.00140.2021/ASSET/IMAGES/LARGE/AJPREGU.00140.2021_F007.JPEG
- Oberholte, H., Niehof, M., Braubach, P., Fieguth, H. G., Jonigk, D., Pfennig, O., Tschernig, T., Warnecke, G., Braun, A., & Sewald, K. (2021). Cigarette smoke alters inflammatory genes

- and the extracellular matrix — investigations on viable sections of peripheral human lungs. *Cell and Tissue Research*, 387(2), 249. <https://doi.org/10.1007/S00441-021-03553-1>
- Pagliuca, G., Rosato, C., Martellucci, S., De Vincentiis, M., Greco, A., Fusconi, M., De Virgilio, A., Gallipoli, C., Simonelli, M., & Gallo, A. (2015). Cytologic and Functional Alterations of Nasal Mucosa in Smokers: Temporary or Permanent Damage? *Otolaryngology– Head and Neck Surgery*, 152(4), 740–745. <https://doi.org/10.1177/0194599814566598>
- Park, J., Langmead, C. J., & Riddy, D. M. (2020). New Advances in Targeting the Resolution of Inflammation: Implications for Specialized Pro-Resolving Mediator GPCR Drug Discovery. *ACS Pharmacology & Translational Science*, 3(1), 88. <https://doi.org/10.1021/ACSPTSCI.9B00075>
- Petrache, I., & Serban, K. (2023). Emphysema. *Pathobiology of Human Disease: A Dynamic Encyclopedia of Disease Mechanisms*, 2609–2624. <https://doi.org/10.1016/B978-0-12-386456-7.05305-3>
- Phillips, B., Veljkovic, E., Peck, M. J., Buettner, A., Elamin, A., Guedj, E., Vuillaume, G., Ivanov, N. V., Martin, F., Boué, S., Schlage, W. K., Schneider, T., Titz, B., Talikka, M., Vanscheeuwijck, P., Hoeng, J., & Peitsch, M. C. (2015). A 7-month cigarette smoke inhalation study in C57BL/6 mice demonstrates reduced lung inflammation and emphysema following smoking cessation or aerosol exposure from a prototypic modified risk tobacco product. *Food and Chemical Toxicology*, 80, 328–345. <https://doi.org/10.1016/j.fct.2015.03.009>
- Radsel, Z., & Kambc, V. (1978). The influence of cigarette smoke on the pharyngeal mucosa. *Acta Oto-Laryngologica*, 85(1–2), 128–134. <https://doi.org/10.3109/00016487809121433>

- Reh, D. D., Higgins, T. S., & Smith, T. L. (2012). Impact of tobacco smoke on chronic rhinosinusitis: a review of the literature. *International Forum of Allergy & Rhinology*, 2(5), 362–369. <https://doi.org/10.1002/alr.21054>
- Renne, R. A., & Gideon, K. M. (2006). Types and Patterns of Response in the Larynx Following Inhalation. *Toxicologic Pathology*, 34(3), 281–285. <https://doi.org/10.1080/01926230600695631>
- Renne, R., Brix, A., Harkema, J., Herbert, R., Kittel, B., Lewis, D., March, T., Nagano, K., Pino, M., Rittinghausen, S., Rosenbruch, M., Tellier, P., & Wohrmann, T. (2009). Proliferative and Nonproliferative Lesions of the Rat and Mouse Respiratory Tract. *Toxicologic Pathology*, 37(7_suppl), 5S-73S. <https://doi.org/10.1177/0192623309353423>
- Services, U. S. D. of H. and H., Prevention, C. for D. C. and, Promotion, N. C. for C. D. P. and H., & Health, O. on S. and. (2014). *The Health Consequences of Smoking—50 Years of Progress*. Centers for Disease Control and Prevention (US). <https://doi.org/NBK179276>
- Shannon, P., Markiel, A., Ozier, O., Baliga, N. S., Wang, J. T., Ramage, D., Amin, N., Schwikowski, B., & Ideker, T. (2003). Cytoscape: a software environment for integrated models of biomolecular interaction networks. *Genome Research*, 13(11), 2498–2504. <https://doi.org/10.1101/GR.1239303>
- Song, Q., Chen, P., & Liu, X. M. (2021). The role of cigarette smoke-induced pulmonary vascular endothelial cell apoptosis in COPD. *Respiratory Research* 2021 22:1, 22(1), 1–15. <https://doi.org/10.1186/S12931-021-01630-1>
- Sopori, M. (2002). Effects of cigarette smoke on the immune system. *Nature Reviews Immunology*, 2(5), 372–377. <https://doi.org/10.1038/nri803>

- Spada, S., Tocci, A., Di Modugno, F., & Nisticò, P. (2021). Fibronectin as a multiregulatory molecule crucial in tumor matrisome: from structural and functional features to clinical practice in oncology. *Journal of Experimental & Clinical Cancer Research : CR*, 40(1), 102. <https://doi.org/10.1186/S13046-021-01908-8>
- Strzelak, A., Ratajczak, A., Adamiec, A., & Feleszko, W. (2018). Tobacco Smoke Induces and Alters Immune Responses in the Lung Triggering Inflammation, Allergy, Asthma and Other Lung Diseases: A Mechanistic Review. *International Journal of Environmental Research and Public Health*, 15(5). <https://doi.org/10.3390/IJERPH15051033>
- Szklarczyk, D., Kirsch, R., Koutrouli, M., Nastou, K., Mehryary, F., Hachilif, R., Gable, A. L., Fang, T., Doncheva, N. T., Pyysalo, S., Bork, P., Jensen, L. J., & Von Mering, C. (2023). The STRING database in 2023: protein-protein association networks and functional enrichment analyses for any sequenced genome of interest. *Nucleic Acids Research*, 51(D1), D638–D646. <https://doi.org/10.1093/NAR/GKAC1000>
- Vineis, P., Alavanja, M., Buffler, P., Fontham, E., Franceschi, S., Gao, Y. T., Gupta, P. C., Hackshaw, A., Matos, E., Samet, J., Sitas, F., Smith, J., Stayner, L., Straif, K., Thun, M. J., Wichmann, H. E., Wu, A. H., Zaridze, D., Peto, R., & Doll, R. (2004). Tobacco and Cancer: Recent Epidemiological Evidence. *JNCI: Journal of the National Cancer Institute*, 96(2), 99–106. <https://doi.org/10.1093/JNCI/DJH014>
- Walrath, J. C., Hawes, J. J., Van Dyke, T., & Reilly, K. M. (2010). Genetically Engineered Mouse Models in Cancer Research. *Advances in Cancer Research*, 106, 113. [https://doi.org/10.1016/S0065-230X\(10\)06004-5](https://doi.org/10.1016/S0065-230X(10)06004-5)

Walser, T., Cui, X., Yanagawa, J., Lee, J. M., Heinrich, E., Lee, G., Sharma, S., & Dubinett, S.

M. (2008). Smoking and Lung Cancer: The Role of Inflammation. *Proceedings of the American Thoracic Society*, 5(8), 811. <https://doi.org/10.1513/PATS.200809-100TH>

Widysanto, A., & Mathew, G. (2022). Chronic Bronchitis. In *Essence of Anesthesia Practice E-Book*. StatPearls Publishing. <https://doi.org/10.1016/B978-1-4377-1720-4.00045-5>

Zhou, Y., Zhou, B., Pache, L., Chang, M., Khodabakhshi, A. H., Tanaseichuk, O., Benner, C., &

Chanda, S. K. (2019). Metascape provides a biologist-oriented resource for the analysis of systems-level datasets. *Nature Communications* 2019 10:1, 10(1), 1–10.

<https://doi.org/10.1038/s41467-019-09234-6>

Appendix A

Table 1

Immune cell-related functional enrichments

Term	Enriched genes
Extracellular matrix	Pzp,Ache,Adamts1,Alpl,Entpd1,Chad,Col13a1,Col15a1,Col3a1,Col4a1,Col4a2,Col4a3,Col5a1,Col5a2,Col6a3,Col1a1,Comp,Eln,F2,Fbn1,Fga,Fgf10,Ccn2,Fn1,Gsto1,Igfbp6,Il16,Itih2,Itln1,Krt1,Lama1,Lamb1,Lamb3,Rpsa,Lgals3,Lgals9,Lox,Loxl1,Lrrn1,Lrrn3,Marco,Matn4,Mmp11,Mmp14,Mmp3,Nid2,Ccn3,Ogn,Serpine1,Reg3g,S100a3,Sema3c,Thbs1,Tnc,Tnr,Wnt11,Wnt7a,Col5a3,Angptl4,Aspn,Tril,Loxl4,Ndnf,Rarres2,Gpc2,Muc5b,Lrrc17,Mfap4,Adamts12,Tnxb,Tinagl1,Loxl2,Spon2,Adamts9,Tspan9,Npnt,Cilp,Adamts14,Adamts17,Spon1,Adamts15,Adamts14,Phospho1,Adamts12,Adamts4,Sspo,Tsku,Optc,Lrig2,Fcgbp1,Abi3bp,Prss34,Lgr6,Colq,Kng2,Angptl7,Hmcn2,Aplp1,Atp7a,Bcl3,Cyp1b1,Eng,Foxc2,Gpm6b,Has1,Has3,Hpn,Lmx1b,Cma1,Pdgfra,Spint1,Spint2,Wnt3a,Wt1,Mmp28,Csgalnact1,Sulf1,Sh3pxd2b,Flrt2
Immune receptor activity	C5ar1,Ccr6,Ccr9,Ccr2,Ccr4,Ccr7,Crlf1,Epor,Fcgr1,Gfra2,Cmk1r1,Il10ra,Il12rb2,Il1r1,Il18r1,Il2rb,Il2rg,Il4ra,Il6ra,Il7r,Klrc1,Klrc2,Il1rl1,Mpl,Lilra6,Prlr,Xcr1,Klrc1,Ccl2,Il17re,Cxcr1,Il22ra2,Fcgr4,H2-Eb2,PirA12,Ager,Comp,Eng,Itga4,Itgb3,Kit,Tcap,Thbs1,Zfp36,Grem2,Chrd11,Tsku,Scube3,Tgfb3l,Edar,Fas1,Il11,Il16,Il1a,Lif,Osm,Ccl12,Ccl17,Ccl25,Cxcl15,Cxcl5,Tnfrsf10b,Tnfrsf9,Cd40lg,Gdf15,Tnfrsf12a,Clefl,Ppbp,Tnfrsf13c,Il36g,Gdf6,Cxcl3,Ccl21f,Egr1,Acs11,Hcls1,Hpx,Mt3,Ptpn,Stat4,Syk,Klf6,Nfkbiz,Trem2,Plvap,Oas2,Entrep1,Adm,Adra1b,Adra1a,Bdkrb2,Calcr,Crhr1,Edn1,Ednra,Gata1,Gata2,Itpr1,Slc8a1,Avpr1a,Fzd2,Ghrl,Ffar4,Plcg2,Cacna1i,Kng2,Chrna10,Gng2,Grk5,Itk,Prkcb,Rasgrp2,Vav1,Was,Foxo3,Vav3,Dock2,Rac3,Prex1,Ada,Cacna1d,Ptgdr2,Htr2b,Itgal,Rcan1,Trem11,Tmem38a

Term	Enriched genes
Lymphocyte activation	Ada,Atp7a,Bcl2a1d,Bcl3,Ccr6,Cd2,Ms4a1,Cd37,Cd79a,Ccr9,Ccr7,Cxad r,Efnb1,Egr1,Eomes,Bcl11a,Dtx1,Cd79b,Il18r1,Il2rg,Il4ra,Il6ra,Il7r,Itgal ,Itgam,Itk,Kit,Klrb1c,Ly6d,Ly9,Myb,Myc,Nfil3,Prf1,Prkcb,Ptpn22,Ptprc ,Rasgrp1,Rorc,Satb1,St3gal1,Slfn1,Slfn2,Stat4,Syk,Cd40lg,Txk,Scgb1a1 ,Vav1,Was,Wnt3a,Ikzf1,Ikzf3,Gadd45g,Exo1,Klrk1,Slamf1,Sh2d2a,Ska p2,Elf4,Clcf1,Rsad2,Bcl11b,Tnfrsf13c,Sash3,Slamf7,Clec4g,Dock11,Hd ac9,Nfkbiz,Dock2,Card11,Gpr18,Fcrl1,Plcg2,Bank1,Fcgr4,Nlrc3,Spib,Pr ex1,Trem12,Cdh26,Itgad,Wdfy4,Ccl21f,Ager,C5ar1,Camp,Itgb6,Nr4a3,S nca,Tlr9,Trem2,Hamp,Enpp3,Adgrf5,Adam8,Calcr,Epha2,Sh3pxd2a,Gat a1,Gata2,Junb,Il1rl1,Prtn3,Tfrc,Srp54a,Diaph3,Pir,Fam20c,Tcim,Il12rb2 ,Il1a,Nod2,H2Eb2,Arg2,Bach2,C2,Cd247,Fga,Hc,Il2rb,Inpp5d,Gzmm,R nf125
Positive regulation of cell migration	Adam8,Adamts1,Ager,Atp7a,C5ar1,Ccr6,Cdh5,Ccr2,Ccr7,Col1a1,Cpeb1 ,Cyp1b1,Dapk2,S1pr1,Edn1,Ednra,Egfr,Egr1,Epha2,Epha4,Erb4,F7,Fg a,Fgf10,Fgfbp1,Foxc2,Fn1,Gata2,Cmklr1,Hspa5,Hspb1,Il1a,Il1r1,Ins13,I tga4,Itgb3,Kit,Lamb1,Lcn2,Lgals3,Lgals9,Mmp14,Mmp3,Myc,Nfe2l2,N r4a3,Ntf3,Ntrk3,Pdgfa,Pdgfra,Pdgfrb,Pecam1,Pik3c2a,Serpine1,Ptafr,Ptg s2,Ptprc,Ccl12,Ccl17,Ccl25,Sema3c,Sema4c,Sema7a,Slc8a1,Thbs1,Tnfa ip6,Wnt7a,Ets1,Map3k3,Slamf1,Rab25,Cldn13,Ppbbp,Trem1,S100a14,Rr as2,Atoh8,Rarres2,Daam2,Plet1,Clasp1,Hdac9,Rhoj,Fgf16,Cemip,Akap1 2,Trem2,Plvap,Gpnmb,Fam110c,Nckap11,Mylk,Prr5,Lyve1,Synpo2,Fer mt2,Plcg2,Ssh2,Dock4,Jcad,Fam107a,Prex1,Cass4,Lgr6,Glipr2,Smim22, Ccl21f,Artn,Ccr4,Il16,Scg2
Positive regulation of cytokine production	Adam8,Ager,Bcl3,Brcal,C5ar1,Cd2,Ccr2,Ccr7,Camp,Cyp1b1,Egr1,Hc, Hspb1,Htr2b,Il12rb2,Il16,Il1a,Il1r1,Il18r1,Il4ra,Il6ra,Itk,Kit,Lgals9,Lpl,I l1rl1,Ly9,Myb,Nr4a3,Osm,Pde4b,Serpine1,Ptafr,Ptgs2,Ptpn22,Ptprc,Ras grp1,Rel,Sema7a,Sod1,Syk,Thbs1,Cd40lg,Txk,Wnt11,Wnt3a,Mapk13,K lrk1,Slamf1,Mefv,Zbtb20,Clec4n,Rsad2,Arrdc4,Inava,C1qtnf4,Hilpda,T

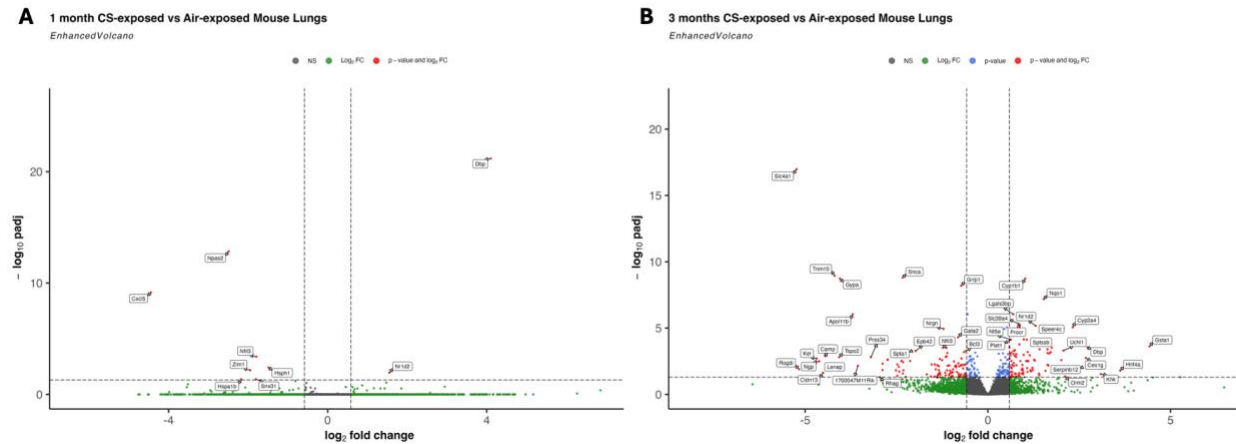
Term	Enriched genes
	nfrsf13c,Sash3,Usp50,Chia1,Tlr9,Akap12,Trem2,Spon2,Card11,Arid5a,I l36g,Nlrp3,Afap1l2,Plcg2,Setd2,Sulf1,Oas2,Nod2,Nlrp1b,Arg2,Tspo,Gst p2,Gstp1,Zfp36,Elf4,Ghrl,Errfi1,Gpnmmb,Gpr18,Nlrc3
Regulation of chemotaxis	Ager,Artn,Bst1,C5ar1,Ccr6,Ccr2,Ccr4,Ccr7,Dapk2,S1pr1,Edn1,Ednra,F 7,Fgf10,Fn1,Cmklr1,Gstp2,Gstp1,Hc,Mst1,Hspb1,Il16,Ccn3,Ntf3,Ntrk3, Pdgfra,Pdgfrb,Serpine1,Dusp1,Scg2,Thbs1,Tnfaip6,Wnt3a,Slamf1,Stap1 ,Pbbp,Trem1,S100a14,Rarres2,Tubb2b,Fgf16,Trem2,Nckap1l,Gpr18,M mp28,Rin3,Nod2,Ccl21f,Ada,Adam8,Gcsam,Il1a,Il1r1,Itga4,Itgb3,Lgals 3,Lgals9,Mmp14,Pecam1,Ptafr,Ptpn22,Ccl12,Ccl25,Gdf15,Chst4,Plvap, Lyve1,Rac3
Regulation of inflammatory response	Ada,Adam8,Ager,Bst1,Cdh5,Clock,Ccr2,Ccr7,Cnr1,Fanca,Fcgr1,Ggt1,G px1,Gpx2,Gstp1,Il10ra,Il16,Il1r1,Krt1,Lgals9,Lpl,Il1rl1,Cma1,Ccn3,Os m,Serpine1,Proc,Ptgs2,Reg3g,Sema7a,Snca,Sod1,Tnc,Tnfaip6,Pglyrp1,S cgb1a1,Zfp36,Ets1,Nt5e,Mefv,Elf4,Clcf1,Stap1,Ghrl,Uaca,C2cd4b,Nfkb iz,Tlr9,Trem2,Pik3ap1,Hamp,Ffar4,Pde2a,Enpp3,Nlrp3,Nr1d1,Plcg2,Il2 2ra2,Adamts12,Cd200r4,Siglecg,Nod2,Nlrc3,Nr1d2,Nlrp1b,Arg2,Epha4, F2,Fga,Gstp2,Hc,Pdgfa,Pdgfra,Pim1,Prkg1,Dusp1,Thbs1,Tnr,Wnt3a,Cla sp1,Gpr18,Mmp28,Dtx4,Tspan8,Rin3,Xylt1,Lrig2,Kng2

Note: Table displaying the immune-related enriched terms and genes after Metascape GO and KEGG pathway database enrichment analysis.

Figure 1

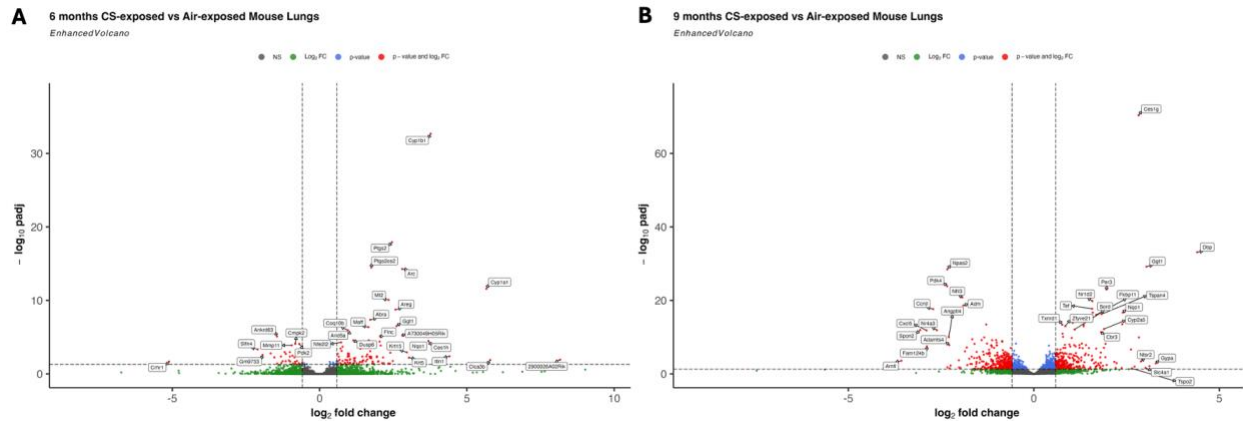
Note. Differential expression analysis revealed eight DEGs between one-day CS-exposed and control groups (**A**). Five upregulated and three downregulated genes were recognized as differentially expressed in response to CS exposure. At day seven, 1031 DEGs with 491 upregulated and 540 downregulated genes were identified between both groups (**B**). The volcano plots here indicate the significant DEGs as red dots.

Figure 2

Differential expression analysis at 1 and 3 months after CS exposure

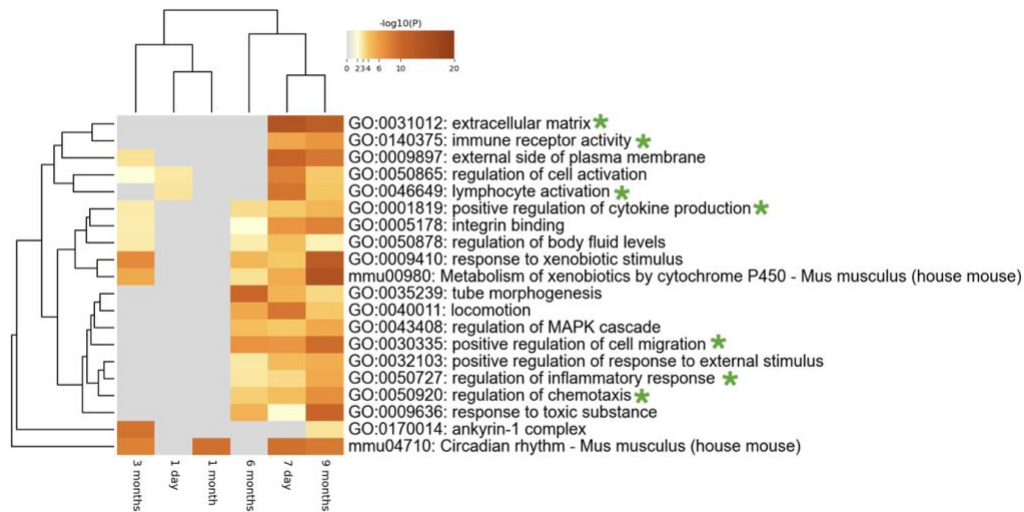
Note. Differential expression analysis revealed nine DEGs between one-month CS-exposed and control groups (A). Two genes showed increased expression, while seven genes exhibited decreased expression. At three months, 190 DEGs with 90 upregulated and 100 downregulated genes were identified between both groups (B). The volcano plots here indicate the significant DEGs as red dots.

Figure 3

Differential expression analysis at 6 and 9 months after CS exposure

Note. Differential expression analysis revealed 121 DEGs (92 upregulated and 29 downregulated) between six months of exposure to CS and control groups (**A**). At nine months, 677 DEGs with 312 upregulated and 365 downregulated genes were identified between both groups (**B**). The volcano plots here indicate the significant DEGs as red dots.

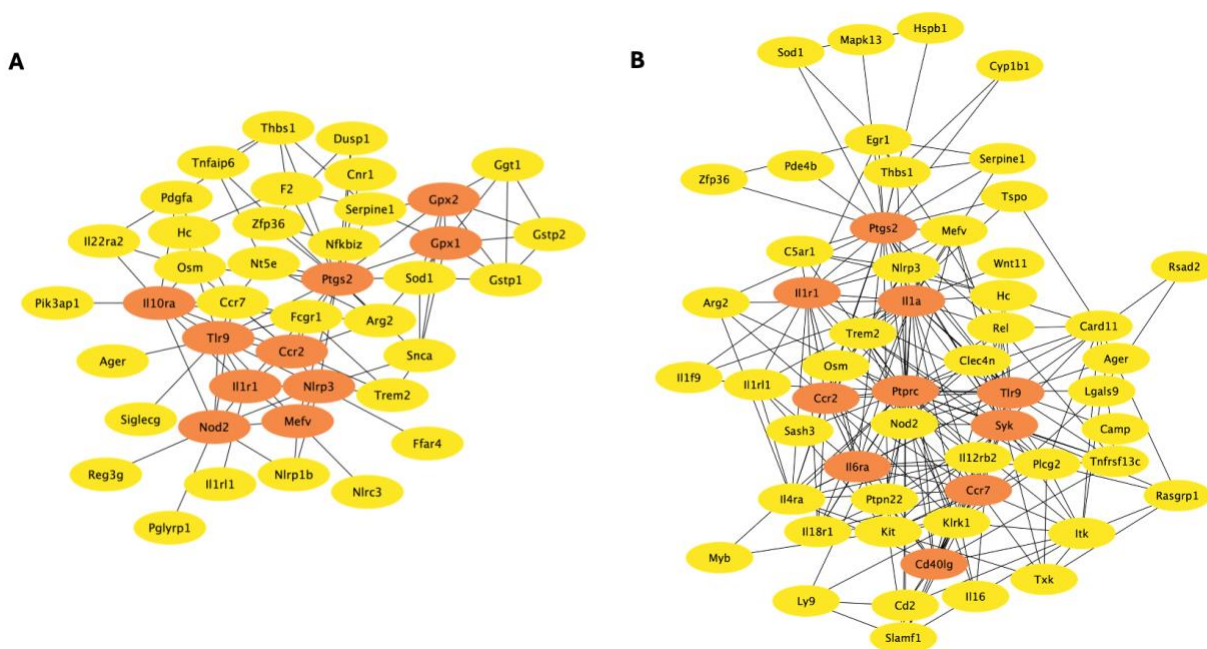
Figure 4

Comparative functional enrichment analysis

Note. Comparative functional enrichment analysis of significant DEGs across all experimental time points was conducted using Metascape. The analysis revealed substantial modulation of various biological mechanisms, mainly immune cell functions and mechanisms, at the longer time points of six- and nine-months following CS exposure. Key findings include changes related to the extracellular matrix, immune receptor activity, lymphocyte activation, positive regulation of cell migration, positive regulation of cytokine production, regulation of chemotaxis, and regulation of inflammatory responses, as marked by green asterisks in the heat map. In contrast, earlier time points did not show significant immune modulation, except for some responses observed on day seven after CS exposure.

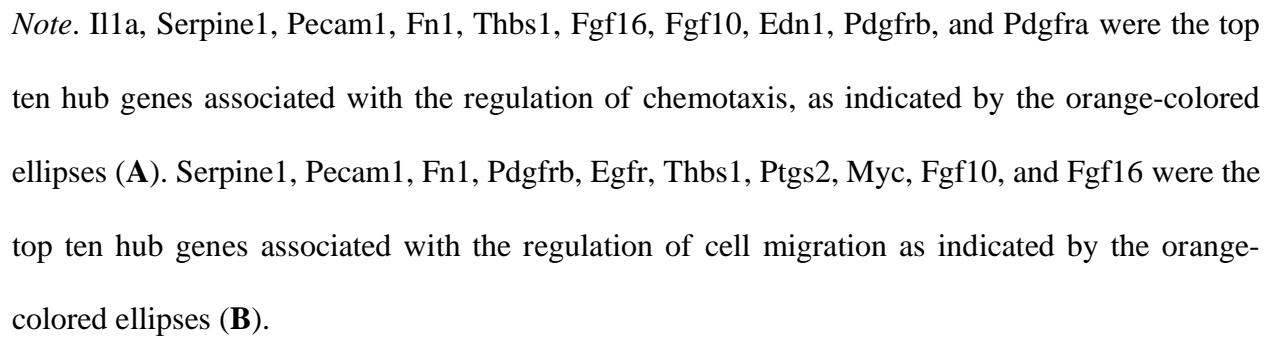
Figure 5

Top ten hub genes in the regulation of inflammation and cytokine production PPIs

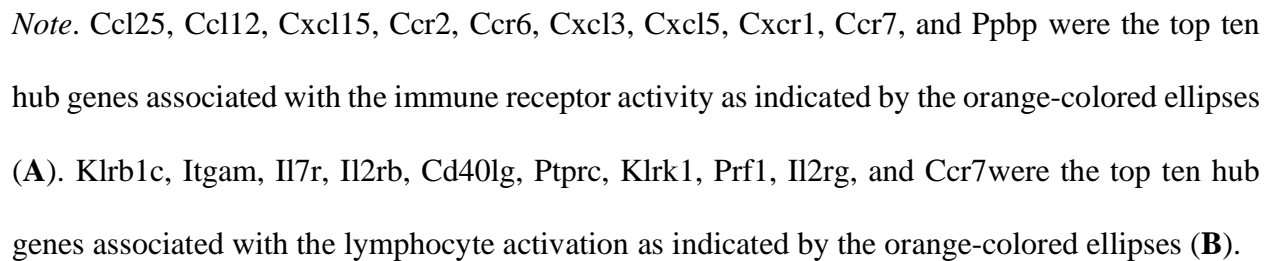


Note. Gpx1, Gpx2, Ptgs2, Ccr2, Nlrp3, Mefv, Il1r1, Nod2, Tlr9, and Il10ra were the top ten hub genes associated with the regulation of inflammatory response as indicated by the orange-colored ellipses (A). Ptgs2, Il1r1, Il1a, Ccr2, Ptpnc, Tlr9, Syk, Il6ra, Ccr7, and Cd40lg were the top ten hub genes associated with the regulation of cytokine production as indicated by the orange-colored ellipses (B).

Top ten hub genes in the regulation of chemotaxis and cell migration PPIs



Top ten hub genes in the immune receptor activity and lymphocyte activation PPIs



Top ten hub genes in the extracellular matrix PPI

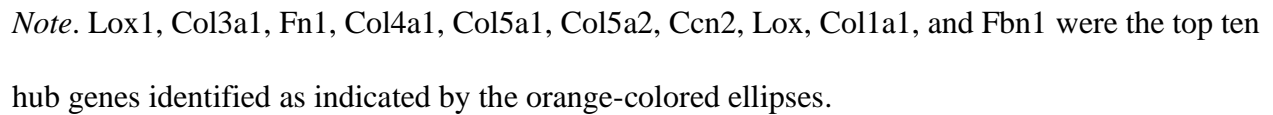
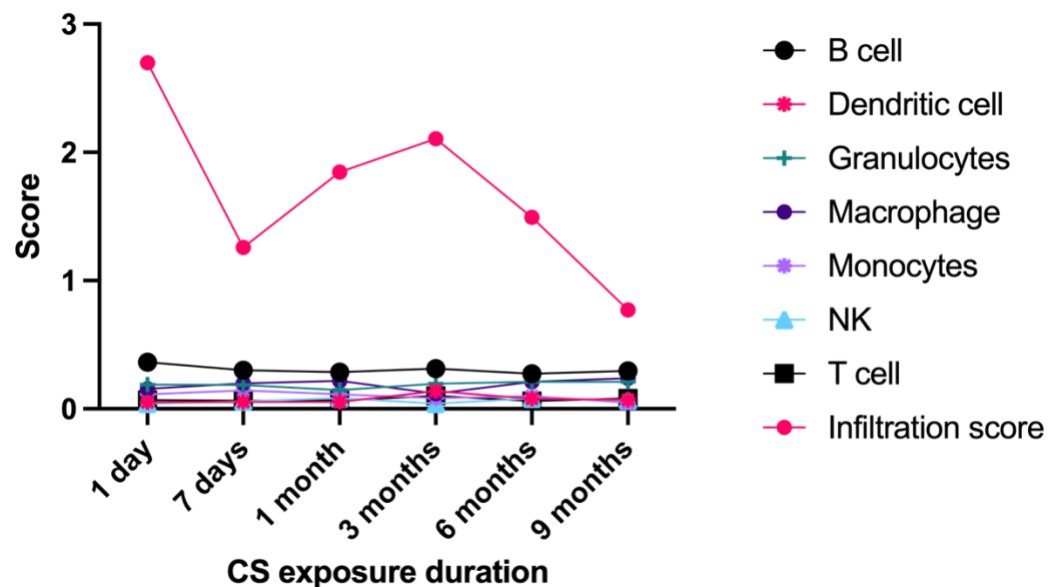


Figure 9

Temporal dynamics of CS-induced immune cell responses in mouse lungs



Note. Analysis of immune cell composition utilizing ImmuneCellAI-mouse, based on expression datasets obtained from the lungs of mice exposed to CS, revealed no significant differences across various exposure time points: one day, seven days, and three, six, or nine months. Assessment of computed immune cell infiltration scores indicated a transient increase following one day of CS exposure, which subsequently declined with extended exposure durations.